Sun-Avoidance Slew Planning Algorithm with Pointing and Actuator Constraints (AAS 10-801)

AIAA/AAS Astrodynamics Specialist Conference, Portland, ME, 11– 15 August 2019

Mohammad. A. Ayoubi[1] Junette Hsin[2]

[1]Associate Professor, Department of Mechanical Engineering, Santa Clara University,
[2]Engineer, Dynamics and Control Analysis Group, Maxar Space Solutions (Formerly Space Systems/Loral)

Outlines

Introduction

1. Literature review

Sun-Avoidance Slew (SAS) Algorithm

Problem Statement:

Given: ${}_{\mathcal{N}}\hat{P}_i$, ${}_{\mathcal{N}}\hat{P}_f$, ${}_{\mathcal{N}}\hat{S}$, ${}_{\mathcal{G}}\hat{P}$, ϵ_p, ${}^{\mathcal{N}}q^{\mathcal{G}}$, ${}^{\mathcal{N}}_{\mathcal{G}}\omega^{\mathcal{G}}(t_i)$, and ${}^{\mathcal{N}}_{\mathcal{G}}\omega^{\mathcal{G}}(t_f)$.

Assumption: The spacecraft is rigid.

Find:

1. A sequence of slew maneuvers to avoid sun vector.
2. the commanded angular velocity, angular acceleration, and quaternion profiles.

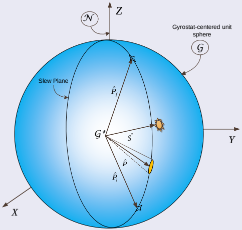

Sun-Avoidance Slew (SAS) Algorithm

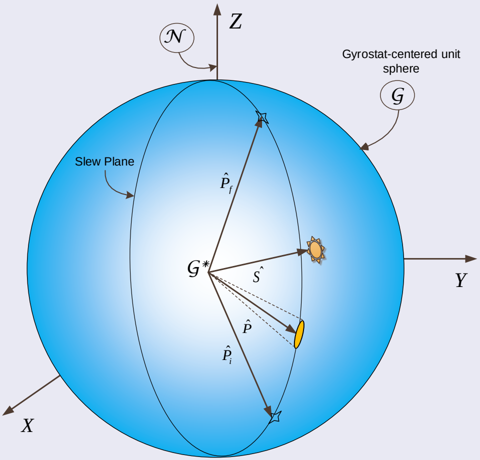

Figure: The gyrostat-centered unit sphere.

Sun-Avoidance Slew (SAS) Algorithm

Nomenclature

- $\mathcal{G}$ frame: Unit sphere attached to the gyrostat.
- $\mathcal{N}$: frame: The Newtonian frame fixed in the inertial space.
- ${}_{\mathcal{G}}\hat{P}$: Unit vector along the bore sight of payload in the $\mathcal{G}$ frame.
- ${}_{\mathcal{G}}\hat{P}_i$: Unit vector of the initial point in the $\mathcal{G}$ frame.
- ${}_{\mathcal{G}}\hat{P}_f$: Unit vector of the final point in the $\mathcal{G}$ frame.
- ${}_{\mathcal{N}}\hat{S}$: Unit vector of the sun vector in the $\mathcal{N}$ frame.
- ϵ_p: Payload half-cone angle.

Numerical Simulations

title

1. Matlab was used to numerically simulate and examine the proposed algorithm.
2. The initial, final, and sun position vectors were randomized for each run.
3. Two cases shown in these slides - one in which the sun angle is greater than 0 from the slew plane, the other in which the sun vector lies directly on the slew plane.
4. Slew angles were found using the methods discussed in the description of the algorithm.

Numerical Simulations

alpha > 0

Table: Slew Angles ϕ_1, ϕ_2, and ϕ_3

ϕ	1	2	3
Angle (rad)	0.29	2.70	0.13
Angle (deg)	16.61	154.80	7.33

Numerical Simulations

alpha > 0

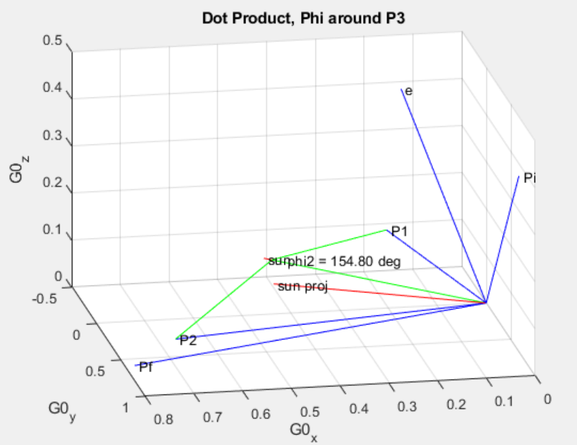

Figure: Chord geometry for finding ϕ_2

Numerical Simulations

alpha > 0

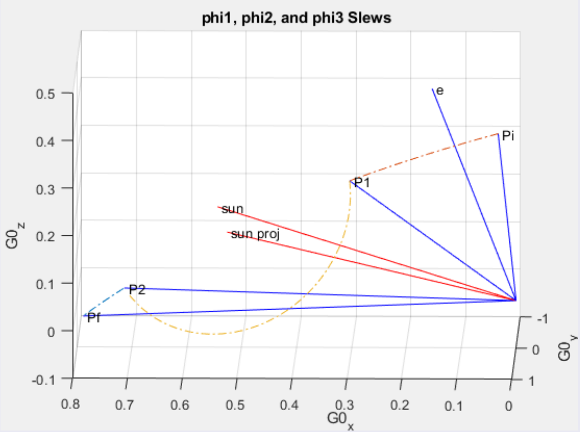

Figure: Attitude Profile of the Entire Slew

Numerical Simulations

alpha > 0

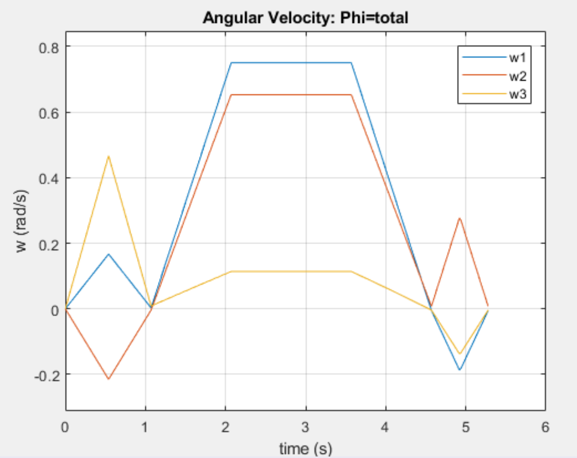

Figure: Angular Velocity in Spacecraft Frame

Numerical Simulations

alpha > 0

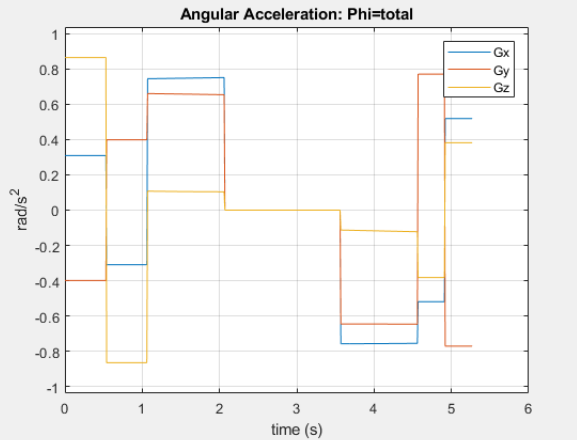

Figure: Angular Acceleration

Numerical Simulations

alpha > 0

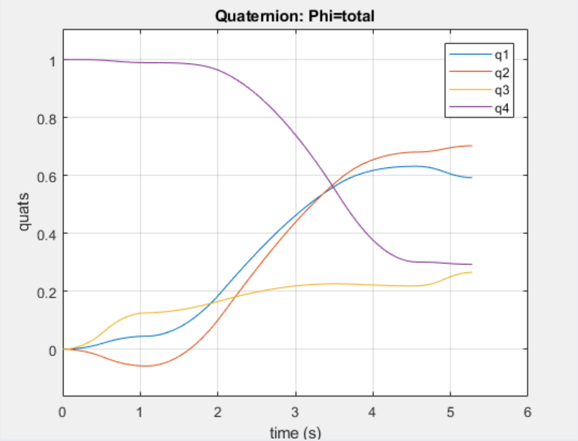

Figure: Quaternion Attitude

Numerical Simulations

alpha > 0

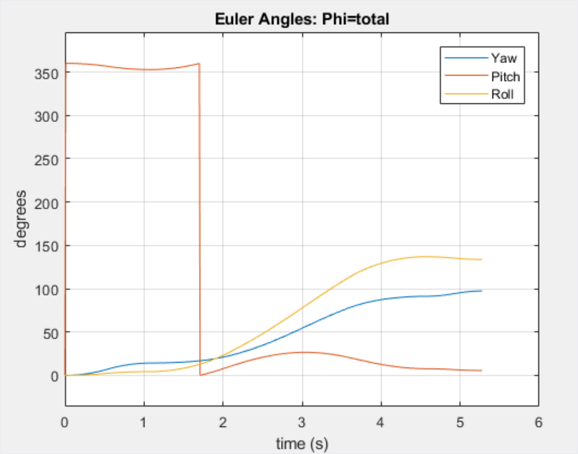

Figure: Attitude in Euler Angles

Numerical Simulations

alpha > 0

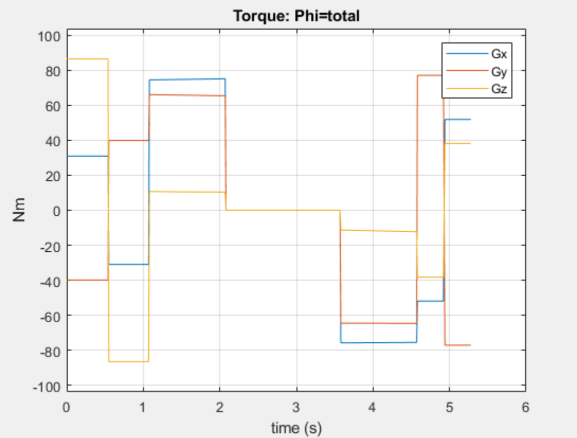

Figure: Torque Applied from Actuator System

Numerical Simulations

alpha $= 0$

Table: Slew Angles ϕ_1, ϕ_2, and ϕ_3

ϕ	1	2	3
Angle (rad)	0.02	3.14	0.00
Angle (deg)	10.80	180	0.00

Numerical Simulations

alpha = 0

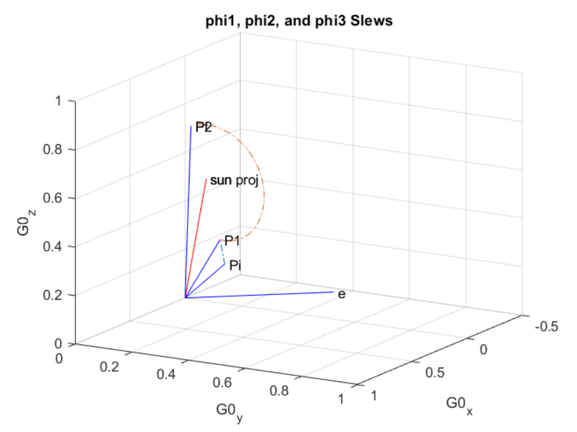

Figure: Attitude Profile of the Entire Slew

Numerical Simulations

alpha = 0

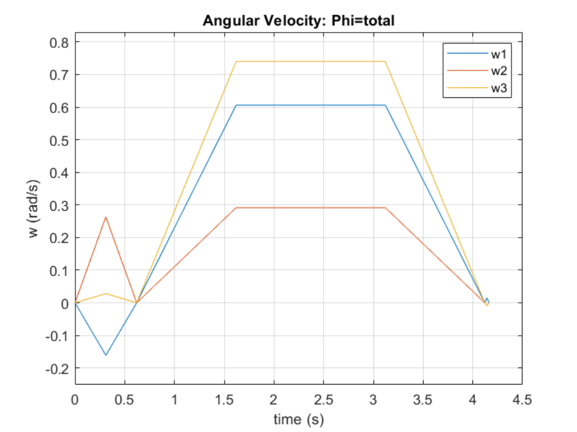

Figure: Angular Velocity in Spacecraft Frame

Numerical Simulations

alpha = 0

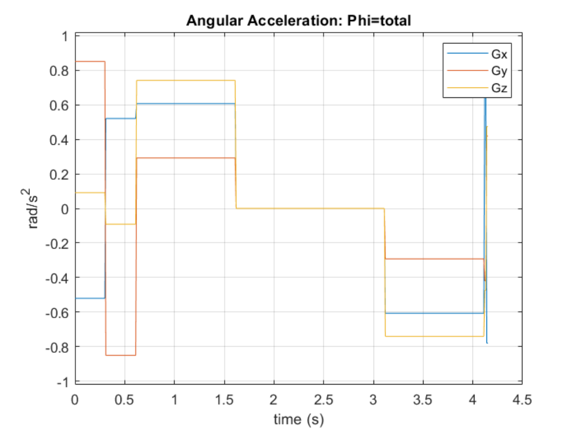

Figure: Angular Acceleration

Numerical Simulations

alpha = 0

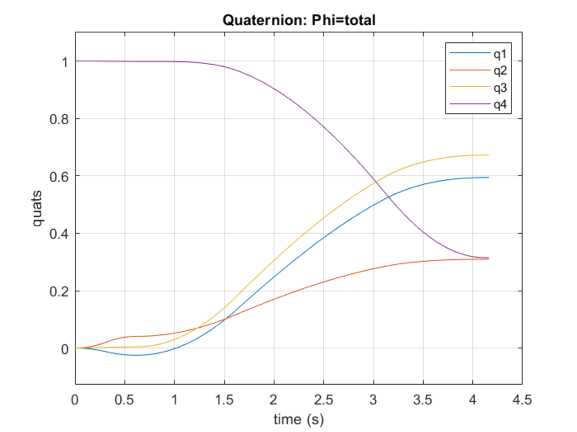

Figure: Quaternion Attitude

Numerical Simulations

alpha = 0

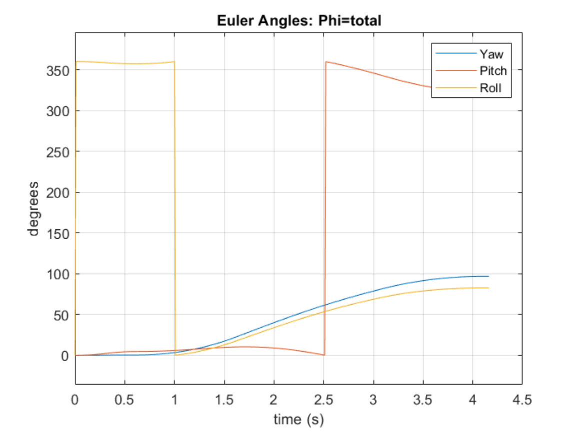

Figure: Attitude in Euler Angles

Numerical Simulations

alpha = 0

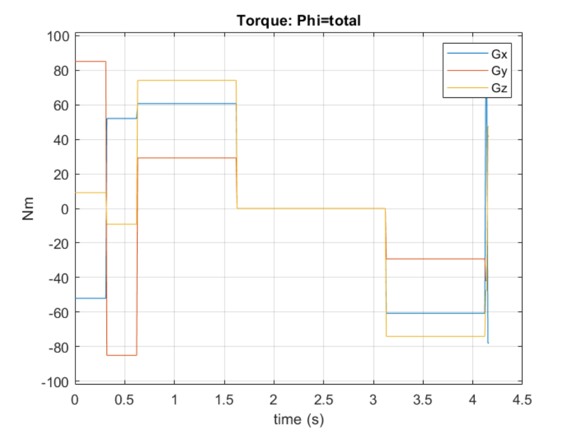

Figure: Torque Applied from Actuator System

Summary and Conclusion

1. Geometric approach for large-angle slew planning with pointing and actuator constraints
2. Assumed that initial and final attitudes, instrument boresight, and sun vector are known
3. Target-frame quaternions, angular velocities, and angular accelerations are derived base on the PMP
4. Limitation is for single sensitive-payload

Acknowledgments

The research has been supported by Maxar Space Solutions (formerly Space Systems/Loral). The second author (Junette Hsin) would like to acknowledge Luke DeGalan for his useful comments.

Q & A

Back-up Slides

Computing the Steering Profiles

Case II: Single-Axis, Agile Slew Maneuver with Acceleration Constraint.

Single-Axis, Agile Slew Maneuver with Acceleration Constraint

Problem Statement:

Consider the optimal control problem described by Eqs.(10), (11), (12), and subject to control constraint

$$C_2 : \ |u = \ddot{\phi}| \leq \ddot{\phi}_{max}. \tag{1}$$

Find: $\phi(t)$, $\dot{\phi}(t)$, and $\ddot{\phi}(t)$.

Single-Axis, Agile Slew Maneuver with Acceleration Constraint

- Angular acceleration about the $\hat{e}$ axis:

$$\ddot{\phi}(t) = \ddot{\phi}_{max}\mathbb{U}(t_0) - 2\ddot{\phi}_{max}\mathbb{U}(t - t_1) \tag{2}$$

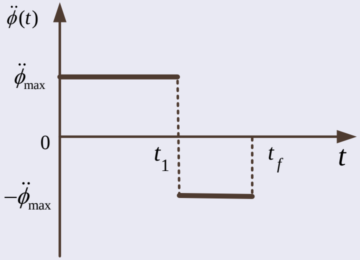

where the switching and the final times are given by

$$t_1 = t_0 - \frac{\dot{\phi}_0}{\ddot{\phi}_{max}} + \frac{\sqrt{\ddot{\phi}^2_{max}(2\ddot{\phi}_{max}\phi_f + \dot{\phi}^2_f + \dot{\phi}^2_0)}}{\sqrt{2}\ddot{\phi}^2_{max}} \tag{3}$$

Single-Axis, Agile Slew Maneuver with Acceleration Constraint

and

$$t_f = t_0 - \frac{\dot{\phi}_f + \dot{\phi}_0}{\ddot{\phi}_{max}} + \frac{\sqrt{2}\sqrt{\ddot{\phi}^2_{max}(2\ddot{\phi}_{max}\phi_f + \dot{\phi}^2_{ef} + \dot{\phi}^2_0)}}{\ddot{\phi}^2_{max}} \quad (4)$$

- Angular velocity about the $\hat{e}$ axis:

$$\dot{\phi}(t) = \dot{\phi}_0 + \ddot{\phi}_{max}(t - t_0)\mathbb{U}(t_0) - 2\ddot{\phi}_{max}(t - t_1)\mathbb{U}(t - t_1) \quad (5)$$

- Angular position about the $\hat{e}$ axis:

$$\begin{aligned}\phi(t) = \dot{\phi}_0(t - t_0) + \ddot{\phi}_{max}\frac{(t - t_0)^2}{2}\mathbb{U}(t_0) \\ - 2\ddot{\phi}_{max}\frac{(t - t_1)^2}{2}\mathbb{U}(t - t_1)\end{aligned} \quad (6)$$

The Agile Sun-Avoidance Slew Maneuver

The First Slew Maneuver:
A single-axis nonrest-to-rest maneuver around the ê

- The BCs:

$$\dot{\phi}(t_0) = \dot{\phi}_0, \phi(t_0) = 0, \dot{\phi}(t_{f1}) = 0, \phi(t_{f1}) = \phi_1. \tag{7}$$

The switching time, t_{11}, and minimum-time, t_{f1}, are

$$t_{11} = t_0 - \frac{\dot{\phi}_0}{\ddot{\phi}_{max}} + \frac{\sqrt{\ddot{\phi}_{max}^2(2\ddot{\phi}_{max}\phi_1 + \dot{\phi}_0^2)}}{\sqrt{2}\ddot{\phi}_{max}^2} \tag{8}$$

$$t_{f1} = t_0 - \frac{\dot{\phi}_0}{\ddot{\phi}_{max}} + \frac{\sqrt{2\ddot{\phi}_{max}^2(2\ddot{\phi}_{max}\phi_1 + \dot{\phi}_0^2)}}{\ddot{\phi}_{max}^2} \tag{9}$$

The $\ddot{\phi}(t)$, $\dot{\phi}(t)$, and $\phi(t)$, can be found by substituting the boundary conditions given by (40) and t_{11} and t_{f1} in to Eqs. (35), (38), and (39), respectively.

The Agile Sun-Avoidance Slew Maneuver

The Second Slew Maneuver: A rest-to-rest maneuver around the sun vector

- The BCs:

$$\dot{\phi}(t_0) = 0, \phi(t_0) = 0, \dot{\phi}(t_{f2}) = 0, \phi(t_{f2}) = \phi_2. \tag{10}$$

The switching time, t_{12}, and the minimum-time, t_{f2}, are

$$t_{12} = t_0 - \frac{\sqrt{\phi_2}}{\ddot{\phi}_{max}} \tag{11}$$

$$t_{f2} = t_0 - \frac{2\sqrt{\phi_2}}{\ddot{\phi}_{max}} \tag{12}$$

The $\ddot{\phi}(t)$, $\dot{\phi}(t)$, and $\phi(t)$, can be found by substituting the boundary conditions given by (43) and t_{12} and t_{f2} in to Eqs. (35), (38), and (39), respectively.

The Agile Sun-Avoidance Slew Maneuver

The Third Slew Maneuver: A single-axis rest-to-nonrest maneuver around the $\hat{e}$

- The BCs:

$$\dot{\phi}(t_0) = 0, \phi(t_0) = 0, \dot{\phi}(t_{f3}) = \dot{\phi}_f, \phi(t_{f3}) = \phi_3. \tag{13}$$

The switching time, t_{13}, and the minimum-time, t_{f3}, are

$$t_{13} = t_0 + \frac{\sqrt{\ddot{\phi}_{max}^2 (2\ddot{\phi}_{max}\phi_3 + \dot{\phi}_f^2)}}{\sqrt{2}\ddot{\phi}_{max}^2} \tag{14}$$

$$t_{f3} = t_0 - \frac{\dot{\phi}_f}{\ddot{\phi}_{max}} + \frac{\sqrt{2\ddot{\phi}_{max}^2 (2\ddot{\phi}_{max}\phi_3 + \dot{\phi}_f^2)}}{\ddot{\phi}_{max}^2} \tag{15}$$

The $\ddot{\phi}(t)$, $\dot{\phi}(t)$, and $\phi(t)$, can be found by substituting the boundary conditions given by (46) and t_{13} and t_{f3} in to Eqs. (35), (38), and (39), respectively.